Metal arrays in structural units based on anion-centered metal tetrahedra

S. V. KRIVOVICHEV* AND S. K. FILATOV

Department of Crystallography, St Petersburg University, University Emb., 7/9 199034 St Petersburg, Russia.
E-mail: sergey@cryst.geol.pu.ru

Abstract

Structural units based on anion-centered metal tetrahedra (XA_4; X = O, N; A = metal) are described as eutactic metal fragments with anions in tetrahedral interstices. In this respect these units may be subdivided into fluorite derivatives and units based on *stellae quadrangulae* (tetrahedral stars). To describe the geometry of the metal arrays a set of tetrahedrally packed metal radii, r_{tp}, is derived for A = Cu, Pb, Bi, and some rare-earth metals from the systematic analysis of the $A \cdots A$ distances within (XA_4) tetrahedra. Analysis of these radii and of the structural geometry of the units shows that the insertion of anions into tetrahedral interstices of the metal fragment causes its expansion and distortions by nonbonded anion–anion repulsions. The main effect is owing to the linkage of (XA_4) tetrahedra *via* edges, which leads to compression of the shared $A \cdots A$ edges and stretching of the unshared edges. The geometry of this effect is described by some empirical expressions. It is suggested that the eutactic arrangement of metal atoms in structural units based on anion-centered metal tetrahedra is caused by the closed-shell metal–metal bonding interactions

1. Introduction

In the past three decades inorganic compounds containing oxygen- and nitrogen-centered metal tetrahedra have received particular attention owing to their interesting structural features and physical properties (see Schleid, 1996; Lulei & Corbett, 1995; Lissner *et al.*, 1996; Lissner & Schleid, 1997; Beck & Simon, 1997; Lulei, 1998*a,b*; Krivovichev, Filatov & Semenova, 1998, and references therein). These compounds are based on tetrahedra having metal atoms (A) at the corners and nonmetal atoms (X) at the centers. Linkage of (XA_4) tetrahedra *via* corners and/or edges produces a large variety of structural units, [X_nA_m].

On the other hand, considerable progress has been made towards a systematic description of crystal structures of oxides, fluorides, nitrides, sulfides, and some other inorganic compounds as 'stuffed' alloys, *i.e.* as metals or alloys with nonmetal atoms inserted into interstitial sites (Hägg, 1931; Pauling, 1960). Recent

developments of this approach have been achieved through the excellent work of O'Keeffe & Hyde (1985, and references therein), Borisov and co-workers (Borisov & Podberezskaya, 1984; Borisov *et al.*, 1998, and references therein) and Vegas and co-workers (Vegas & Isea, 1997, 1998; Isea *et al.*, 1998, and references therein).

Although the use of such a model was often considered useful, its physical basis has only been discussed in a few works. Lebedev (1969) explains the metal-like cation arrangement in inorganic compounds as a consequence of the idea that anions are small and cations are large. As a result, metal atoms are closely packed and anions are located in the interstices of the cation packing (Lebedev, 1970, 1978). In fact, Lebedev used the Bragg–Slater system of atomic radii supplemented by his own crystal-chemical investigations. Lebedev's approach to the ionic radii was criticized in detail by Urusov (1989) on the basis of data on electron density distributions. O'Keeffe & Hyde (1985) noted that in oxides 'the spacing of densely packed cations (which are next-nearest neighbours) depends on their non-bonded rather than their ionic radii'. Borisov & Podberezskaya (1984) explained the closest packings of cations by the tendency of atoms to form a maximally uniform spatial distribution. Vegas and co-workers (Isea *et al.*, 1998, and references therein) demonstrated that in a number of inorganic compounds usually considered in the light of the ionic model, metal atoms form fragments which reproduce both the topology and the interatomic distances of the neutral elements in pure metals. To explain this feature, partial redox processes between metal and nonmetal atoms are assumed (Vegas & Martínez-Cruz, 1995). As a result, it is suggested that the remaining valence electrons are involved in the formation of specific metal–metal bonding interactions. This idea is supported by the theoretical and experimental evidence of attraction between closed-shell ions of the same nominal charge. These closed-shell interactions have been detected between cations (Pyykkö, 1998) as well as between anions (Bader, 1998; Luaña *et al.*, 1999).

The aim of this paper is to analyze metal arrays in structural units based on anion-centered metal tetrahedra by comparison with atom arrangements in pure metals and alloys. It appears that metal arrays in these

chemically distinct compounds are very similar, sometimes even to the identity of the metal–metal interatomic distances. In the paper we shall analyze these facts and discuss possible physical reasons for them.

2. Metal arrays in anion-centered metal tetrahedral units and in metals and alloys: a comparison

2.1. *Cubic eutaxy, fluorite and fluorite derivatives*

We consider first the structures in which the metal arrays correspond to the arrangements of the centers of spheres in close packings. Following O'Keeffe (1977), we call such arrangements *eutactic*. By analogy with close packings, one can subdivide them into hexagonal and cubic *eutaxies* corresponding to the hexagonal and cubic close packings, respectively. It is well known that
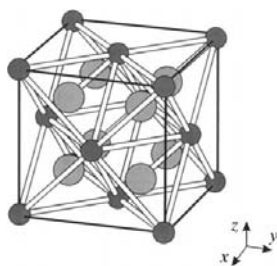

Fig. 1. The crystal structure of fluorite, CaF_2, as a cubic eutaxy of Ca atoms with F atoms in tetrahedral interstices. Metal and nonmetal atoms are shown as small dark gray and large light gray spheres, respectively. The lines connecting the metal atoms serve only to show the metal tetrahedra.

most metal and many alloy structures are organized according to eutactic principles. There are two types of interstitial sites in eutactic arrangements: tetrahedral and octahedral.

Consider the cubic eutaxy. Filling all tetrahedral interstices of this array produces the structure of fluorite, CaF_2, shown in Fig. 1. As was noted by O'Keeffe & Hyde (1985), the parameters of the cubic unit cell of metallic calcium and of fluorite are almost the same (5.588 and 5.463 Å, respectively). There is a number of oxides which may be described as defect fluorite structures (*e.g.* binary rare-earth oxides: Kang & Eyring, 1997, 1998; Adachi & Imanaka, 1998; Vegas & Isea, 1998). Most known types of anion-centered metal tetrahedral units may be also described as derivatives of the fluorite structure. In the following we consider some structural units as examples.

2.1.1. *'(100) derivatives'*. Fig. 2(a) shows the layer obtained from the fluorite framework by cutting parallel to (100). This infinite two-dimensional unit has $[XA]$ stoichiometry and is abundant in metal oxyhalides and oxysulfides, for instance in the so-called Sillén and Aurivillius phases as well as in α,β-PbO. By eliminating different blocks of tetrahedra from this layer distinct 'defect' layers may be obtained; these are shown in Figs. 2(b) and (c). The layer observed in kombatite, $[Pb_{14}O_9](VO_4)_2Cl_4$ (Cooper & Hawthorne, 1994), is of special interest. As can be seen from Fig. 2(c), it has large 'butterfly'-like sevenfold holes. Condensation of two such layers produces the double layer $^2_\infty[O_9Eu_4Pb_6]$ observed in the crystal structure of $[Eu_4Pb_6O_9](PO_4)_2$ recently determined by Palkina *et al.* (1997) and
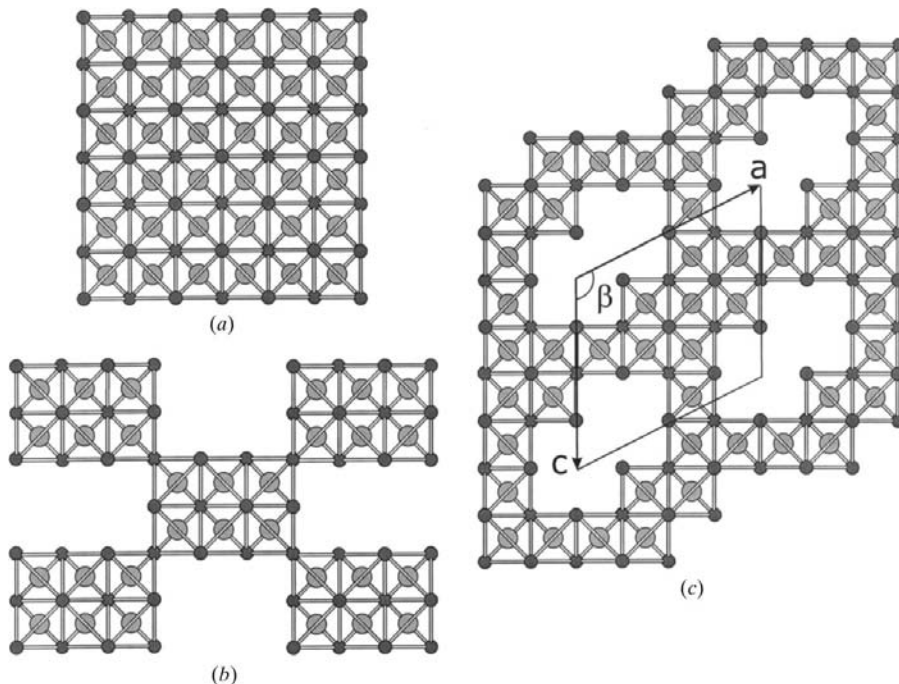

Fig. 2. Structural units obtained by cutting the fluorite structure parallel to the (100) plane (see text and Fig. 1 for details).

Table 1. *Crystal data for kombatite, $[Pb_{14}O_9](VO_4)_2Cl_4$, and $[Eu_4Pb_6O_9](PO_4)_2$*

	Space group	a (Å)	b (Å)	c (Å)	β (°)	Reference
$[Pb_{14}O_9](VO_4)_2Cl_4$	$C2/c$	12.480	14.812	11.134	117.04	(1)
$[Eu_4Pb_6O_9](PO_4)_2$	$C2/c$	12.682	22.566	11.279	118.11	(2)

References: (1) Cooper & Hawthorne (1994); (2) Palkina *et al.* (1997).

described as a complex framework of coordination polyhedra of cations. Table 1 lists the crystal data for both structures and shows that the unit-cell parameters (a, c and β) of the layers are very similar.

There are two ways of obtaining chains from the layer shown in Fig. 2(*a*): cutting parallel to either the [001] or [011] directions in the original fluorite structure. The first way evidently gives *zweier* chains, whereas the second way produces *einer* chains (or their distorted derivatives). Fig. 3 shows the two types of chain observed in crystal structures of inorganic compounds. Table 2 lists example compounds and the identity periods of their chains. A similar method of obtaining chains of oxocentered lanthanum tetrahedra was used by Carre *et al.* (1984) to illustrate the structural diversity of $[OLa_4]$ units in lanthanum oxysulfides. The interesting example of '[011] chains' is shown in Fig. 3(*h*). Its *vierer* variant (*i.e.* with four tetrahedra within the identity period), $_\infty^1[X_3A_5]$, was recently observed in $[Pb_5O_3]O(MoO_4)_2$ (Vassilev & Nihtianova, 1998), whereas its *zweier* analog is present in $[Pb_5O_3]O(SO_4)_2$ (Steele & Pluth, 1998). In these structures there is also one O atom with planar triangular coordination which links $_\infty^1[O_3Pb_5]$ chains into frameworks with large channels which accommodate isolated (MoO_4) or (SO_4) groups.

2.1.2. *'(111) derivatives'.* Another way of cutting the fluorite structure into layers is perpendicular to the

threefold axis, *i.e.* perpendicular to the [111] direction or parallel to the (111) plane. Fig. 4(*a*) shows the double layer $_\infty^2[AX]$ observed in a number of compounds in which A is a rare-earth metal. In fact, this layer represents two eutactic layers of A atoms in which all tetrahedral interstices are filled by O atoms. Octahedral interstices are, as a rule, 'empty', but in some cases they are partially occupied by O atoms (*e.g.* in $[Ce_2O_2]O_{0.5}S$; Mauricot *et al.*, 1997).

Fig. 4(*b*) shows a $_\infty^2[X_2A_5]$ layer of (XA_4) tetrahedra based on the kagomé or (3.6.3.6) net (Fig. 4*c*). This layer has been observed in averievite, $[Cu_5O_2](VO_4)_2 \cdot MX$ (Starova *et al.*, 1997) and in $[Pb_2Cu_3O_2](NO_3)_2(SeO_3)_2$ (Effenberger, 1986), in which each triangle of kagomé $_\infty^2[Cu]$ net is capped by Cu or Pb atoms, respectively. The simple kagomé net is widely observed in alloys, *e.g.* for Cu atoms in $CaCu_5$, Zn atoms in $MgZn_2$ and $CaZn_5$, and Fe atoms in W_6Fe_7 (Kripyakevich, 1977; O'Keeffe & Hyde, 1980). The capped kagomé net is observed in Zr_4Al_3, in which the $_\infty^2[Al]$ net is capped by Zr atoms, but, in contrast to the compounds cited above, all Zr corners of 'empty' (Al_3Zr) tetrahedra point in the same direction relative to the layer plane (Kripyakevich, 1977). The layer shown in Fig. 4(*b*) may also be described as built by successive linking of single *zweier* chains $_\infty^1[X_2A_5]$ as shown in Fig. 4(*d*). These chains have also been recognized in a number of inorganic compounds (for details see Krivovichev, Filatov, Semenova & Rozhdestvenskaya, 1998). Double chains of this type (Fig. 4*e*) are present in stoiberite, $[Cu_5O_2](VO_4)$ (Shannon & Calvo, 1973). Three distinct chains with alternation of edge and corner sharing are shown in Figs. 4(*f*), (*g*) and (*h*). They are observed in georgbokiite, $[Cu_5O_2](SeO_3)_2Cl_2$ (Krivovichev *et al.*, 1999), $[Pb_2O]_2[Pb_7O_3]O(TO_4)[T_2O_7]$ (T = Si, Ge; Kato, 1982; Kato *et al.*, 1995) and freedite, $[Pb_8O_3]Cu(AsO_3)_2Cl_5$ (Pertlik, 1987), respectively. It should be noted that the description of $[Pb_2O]_2[Pb_7O_3]O(TO_4)[T_2O_7]$ (T = Si, Ge) compounds as built of two types of chains of oxocentred Pb tetrahedra seems to be more correct than that based on chains and layers of (OPb_4) tetrahedra given earlier (Krivovichev, Filatov & Semenova, 1998).

2.1.3. *Finite units.* Finite complexes of anion-centered metal tetrahedra which may be described as fluorite derivatives are shown in Figs. 5(*a*)–(*g*) (example compounds are collected in Table 3). The most interesting example is the unit known as *stella octangula* (O'Keeffe & Hyde, 1996) consisting of 14 metal atoms (Fig. 5*d*). It may be described as an all-face-capped
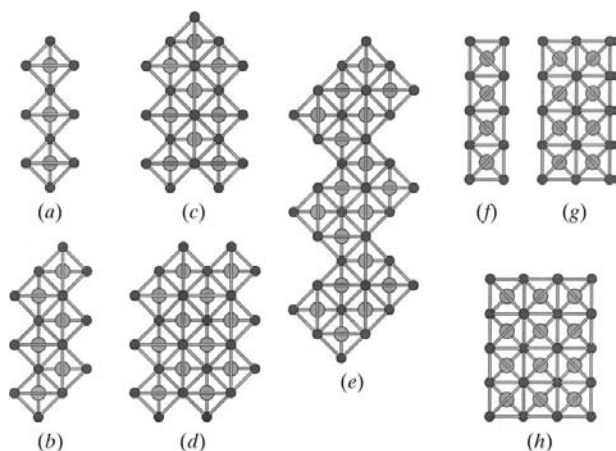

Fig. 3. Chains of anion-centered metal tetrahedra obtained by cutting the fluorite structure parallel to the (100) plane and the [011] (*a*)–(*e*) and [100] (*f*)–(*h*) directions in the original fluorite structure (see text, Table 2, and Fig. 1 for details).

Table 2. *Examples of inorganic compounds containing chains of anion-centered metal tetrahedra*

I_{chain} is the identity period (Å), t is the direction of chain extension, P is the periodicity and M is the multiplicity.

Chain	Figure	I_{chain}	t	P	M	Compound	Reference
$^1_\infty[XA_3]$	3(a)	3.730	c	1	1	$[Y_3O](OH)_5Cl_2$	(1)
		3.948	b	1	1	$[Sm_3N]S_3$	(2)
$^1_\infty[XA_2]$	3(b)	3.801	b	1	2	$[Dy_2O]S_2$-I	(3)
		4.030	b	1	2	$[La_2O][LaGaS_5]$	(4)
		3.916	b	1	2	$[Sm_2N]_2S_3$	(5)
$^1_\infty[X_3A_5]$	3(c)	4.060	c	1	3	$[La_5O_3]_2In_6S_{17}$	(6)
						$[(Fe^{2+}, Fe^{3+}, Ti)_3O_2][As_2O_5]$,	
$^1_\infty[X_2A_3]$	3(d)	3.252	b	1	4	fetiasite	(7)
$^1_\infty[X_3A_5]$	3(e)	15.330	a	4	2	$[Pb_5O_3]O(MoO_4)_2$	(8)
$^1_\infty[XA_2]$	3(f)	6.140	c	2	1	$[Gd_2N]Cl_3$	(9)
						$[Pb_2O](SO_4)$,	
		5.698	b	2	1	lanarkite	(10)
		11.950	(a + b)/2	4	1	$[La_8N_3O]Br_{13}$	(11)
		11.707	b	4	1	$Na_2[Pr_4NO]Br_9$	(12)
$^1_\infty[X_2A_3]$	3(g)	5.954	b	2	2	$[Pb_3O_2]I_2$	(13)
		5.173	b	2	2	$[BiCu_2O_2](PO_4)$	(14)
		5.508	c	2	2	$Gd[Gd_3O_2](WO_5)_2$	(15)
$^1_\infty[X_3A_4]$	3(h)	5.852	c	2	3	$[La_4O_3][AsS_3]_2$	(16)
		5.659	c	2	3	$[Ho_4O_3][Mo_4O_8]$	(17)

References: (1) Klevtsova *et al.* (1967); (2) Lissner & Schleid (1993); (3) Schleid (1991); (4) Jaulmes *et al.* (1983); (5) Lissner & Schleid (1994); (6) Gastaldi *et al.* (1982); (7) Graeser *et al.* (1994); (8) Vassilev & Nihtianova (1998); (9) Schwanitz-Schüller & Simon (1985); (10) Sahl (1970); (11) Lulei (1998b); (12) Lulei *et al.* (1995); (13) Kramer & Post (1985); (14) Abraham *et al.* (1994); (15) Tyulin & Efremov (1987); (16) Palazzi & Jaulmes (1981); (17) Gougeon *et al.* (1991).

octahedron. In this metal cage there are nine interstitial cavities, one octahedral and eight tetrahedral. If all the tetrahedra are filled by X atoms, an $[X_8A_{14}]$ isolated unit is obtained which, however, is not known so far. But if these units are linked by corner sharing, one obtains the $^3_\infty[X_4A_5]$ framework (Fig. 6a) which has been observed in $[CdY_4O_4](MoO_4)_3$ (Bourdet *et al.*, 1982) and $[Nd_5O_4](MoO_4)_3$ (Hubert *et al.*, 1973). Frameworks of *stellae octangulae* built from cation-centered (AS_4) sulfur tetrahedra are known in pentlandite and djerfischerite-like compounds (Belov, 1976; Halet & Saillard, 1997); however, their topology is different from that found in the frameworks shown in Fig. 6(a). There are some derivatives of *stella octangula*. Fig. 5(e) shows the $[X_6A_{12}]$ unit recently discovered by Braun *et al.* (1995, 1996) in $A[Th_{12}N_6]X_{29}$ (A = Li–Rb; X = Cl, Br). This unit is easily obtained from *stella octangula* by removal of two (XA_4) tetrahedra. It is worth noting that
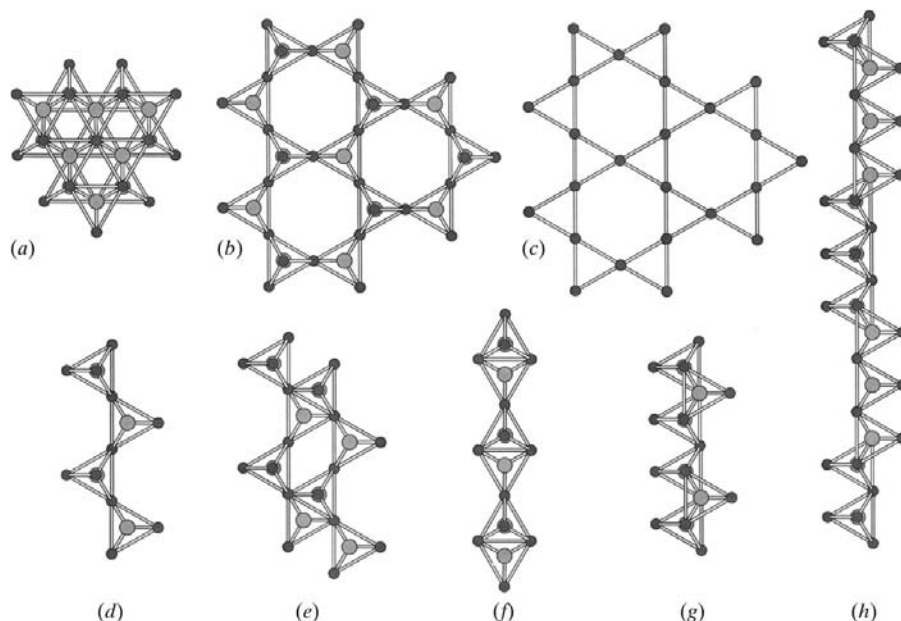

Fig. 4. Structural units obtained by cutting the fluorite structure parallel to the (111) plane (see text and Fig. 1 for details).

Table 3. *Examples of inorganic and metal-organic compounds containing finite units based on anion-centered metal tetrahedra*

Formula	Figure	Compound	Reference
$[XA_4]$	5(*a*)	$(A_4O)S_4Cl_2$ (A = La–Nd)	(1)
		$(Pr_4N)S_3Cl_3$	(2)
$[X_2A_7]$	5(*b*)	$Pb_2[Pb_7O_2][Al_8O_{19}]$	(3)
$[X_2A_6]$	5(*c*)	$K_2[Cu_3O](SO_4)_3$	(4)
		$[La_3N]Br_6$	(5)
		$[Pr_3O](GeO_4)(PO_4)$	(6)
$[X_6A_{12}]$	5(*e*)	$A'[Th_{12}N_6]Br_{29}$	(7)
		(A' = alkali metal)	
$[X_4A_{10}]$	5(*f*)	$[Pd_6Cu_4O_4]Cl_{12}(HMPA)_4$	(8)
		$[Me_4N][[Mn_{10}O_4](biphen)_4Cl_{12}]$	(9)
$[X_8A_{13}]$	5(*g*)	$[Zr_{13}O_8](OCH_3)_{36}$	(10)
$[X_4A_8]$	5(*h*)	$A'[Pb_8O_4]Br_9$ (A' = Pb, Tl)	(11)
		$[Sn_8O_4](SO_4)_4$	(12)
		$[Pb_8O_4]_2[Si_{25}Al_{23}O_{96}]$	(13)

References: (1) Schleid & Lissner (1994); (2) Schleid & Meyer (1996); (3) Ploetz & Müller-Buschbaum (1981); (4) Starova *et al.* (1991); (5) Lulei (1998*b*); (6) Dzhurinskii *et al.* (1991); (7) Braun *et al.* (1995, 1996); (8) Hosokawa *et al.* (1996); (9) Goldberg *et al.* (1995); (10) Wells (1984); (11) Keller (1982, 1983); (12) Lundgren *et al.* (1982); (13) Yeom *et al.* (1997).

$A[Th_{12}N_6]X_{29}$ is really a cluster compound having two electrons left for the formation of metal–metal bonds. Fig. 5(*f*) shows an $[M_{10}]$ metallic cage which has four tetrahedral and one octahedral interstices. Filling of all the former by X atoms results in $[X_4M_{10}]$ units observed in metal-organic compounds (see Table 3). Housecroft (1997) described the structures containing $[Os_{10}C]$ and $[Ru_{10}N]$ clusters in which X atoms (C and N) are in the octahedral cavities of the $[M_{10}]$ cages. The eutactic arrangement of the metals is preserved in both variants of interstition.

We have described a number of anion-centered metal tetrahedral units as being derived from the cubic eutaxy of metal atoms in which tetrahedral interstices are filled by anions. There are also inorganic compounds based on units which cannot be represented as blocks of cubic eutaxies, as will be described below.

2.2. *Stella quadrangula and its derivatives*

Stella quadrangula (Tetraederstern, tetrahedral star) is usually represented as a tetrahedron having all the faces capped (Fig. 5*h*). This unit is widely used in the description of complex alloy structures (Nyman & Andersson, 1979; Andersson, 1981; Häussermann *et al.*, 1998) and of cation arrangements in some oxides and fluorides (O'Keeffe & Hyde, 1985; Borisov *et al.*, 1993). However, *stella quadrangula* has also been observed among units based on anion-centered metal tetrahedra. It has five tetrahedral cavities, one central and four peripheral. The stable configuration is obviously that in which only the latter are filled, giving rise to the formula $[X_4A_8]$. Keller (1982, 1983) discovered $[O_4Pb_8]$ *stella quadrangulae* in $A[Pb_8O_4]Br_9$ compounds (A = Pb, Tl). Recently Yeom *et al.* (1997) reported the crystal structure of zeolite X (the synthetic counterpart of faujasite) exchanged with Pb^{II} at pH 6.0 and dehydrated. This zeolite has sodalite cages occupied by $[O_4Pb_8]$ *stella quadrangulae*. An isolated metal tetrahedral star without interstitial atoms is present as a $[Pt_4Ge_4]$ unit in $Na_3Pt_4Ge_4$ (O'Keeffe & Hyde, 1996).

Linking of *stellae quadrangulae via* unshared corners results in the framework shown in Fig. 6(*b*). Metallic arrays with such a structure have been observed for Fe atoms in Fe_3W_3C (Andersson, 1981) and for Na atoms in NaBa (Häussermann *et al.*, 1998). Inorganic compounds

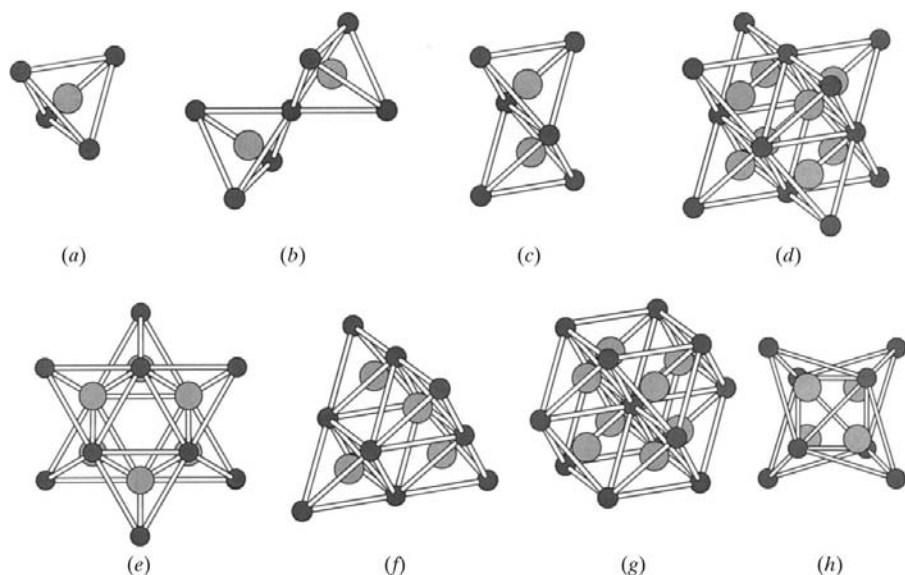*(a)*   *(b)*   *(c)*   *(d)*

(e)   *(f)*   *(g)*   *(h)*

Fig. 5. Finite units based on anion-centered metal tetrahedra (see text, Table 3, and Fig. 1 for details).

Table 4. *Inorganic compounds containing frameworks of corner-sharing interstitially stabilized stellae quadrangulae*

	Space group	a (Å)	Reference
$[Bi_3O_2][Ru_3O_9]$	$Pn\bar{3}$	9.305	(1)
	$Pn\bar{3}$	9.302	(2)
$[Bi_3O_2][GaSb_2O_9]$	$Pn\bar{3}$	9.491	(3), (4)
$[Bi_3O_2][AlSb_2O_9]$	$Pn\bar{3}$	9.490	(4)
$[NaBi_2O_2][Sb_3O_9]$	$Pn\bar{3}$	9.492	(5)
$[La_3O_2][Ru_3O_9]$	$Pn\bar{3}$	9.451	(6)
	$Pn\bar{3}$	9.466	(7)
$[La_3O_2][Ir_3O_9]$	$Pn\bar{3}$	9.499	(8)
$[Pb_2EuO_2][AlO_2]_3$	$Pn\bar{3}m$	9.458	(9)
$[Pb_2GdO_2][AlO_2]_3$	$Pn\bar{3}m$	9.445	(9)
$[Pb_2LuO_2][AlO_2]_3$	$Pn\bar{3}m$	9.349	(10)
$[Pb_2HoO_2][AlO_2]_3$	$Pn\bar{3}m$	9.416	(10)

References: (1) Abraham *et al.* (1975); (2) Facer *et al.* (1993); (3) Sleight & Bouchard (1973); (4) Ismunandar *et al.* (1996); (5) Champarnaud-Mesjard *et al.* (1995); (6) Abraham *et al.* (1978); (7) Cotton & Rice (1978); (8) Abraham *et al.* (1979); (9) Müller-Buschbaum & Werner (1996); (10) Scheikowski & Müller-Buschbaum (1993).

with frameworks of interstitially stabilized *stellae quadrangulae* are listed in Table 4. The most interesting feature of these compounds is that they consist of three interpenetrating frameworks, one built from cation-centered O-atom polyhedra [$(A'O_4)$ or $(A'O_6)$, A' = Al, Ir, Ru, Os] and two symmetry-equivalent ones built from $[O_4A_8]$ *stellae quadrangulae* (Fig. 6b). This feature was recognized for $[A_3O_2][A'_3O_9]$ compounds by Sleight & Bouchard (1973) (see also Abraham *et al.*, 1975; Ismunandar *et al.*, 1996), whereas $[A_3O_2][A'O_2]$ compounds (Scheikowski & Müller-Buschbaum, 1993; Müller-Buschbaum & Werner, 1996) were originally described in terms of cation-centered coordination polyhedra.

3. Structural distortions caused by interstitial anions

3.1. *Anion···anion repulsions and distortion of global geometry*

Most of the models described in §2 are based on ideal eutactic arrangements. Insertion of nonmetal atoms X
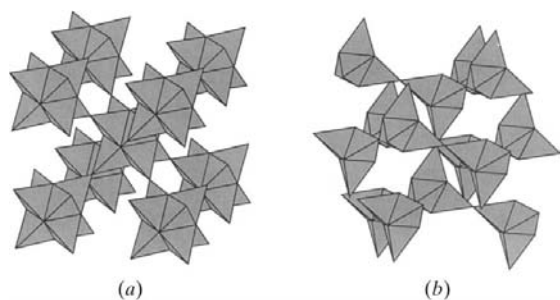
Table 5. *Geometrical parameters of the layers shown in Fig. 7 in the crystal structures of inorganic compounds*

Compound	t' (Å)	t'' (Å)	$t'':t'$	Reference
$[Gd_2O](SiO_4)$	c, 6.730	b, 7.060	1.049	(1)
$[Eu_2O](GeO_4)$	c, 6.854	b, 7.136	1.041	(2)
$[Nd_2O](GeO_4)$	b, 6.980	c, 7.259	1.040	(3)
$[Gd_2O](GeO_4)$	c, 6.838	b, 7.090	1.037	(4)
$Na[Ho_2O]_2(GeO_4)(OH)$	a, 6.705	c, 6.910	1.029	(5)
$[Y_2O]S_2$	c, 6.853	b, 6.885	1.005	(6)
$[Dy_2O]S_2$	c, 6.863	b, 6.911	1.007	(7)
$[Sm_2O]S_2$	c, 6.977	b, 7.062	1.012	(8)
$[Er_2O]S_2$	c, 6.805	b, 6.833	1.004	(9)
$[Tm_2O]S_2$	c, 6.774	b, 6.796	1.003	(9)
$[Yb_2O]S_2$	c, 6.740	b, 6.762	1.003	(9)
$[Hg_2O]I$	c, 6.701	b, 6.981	1.042	(10)

References: (1) Smolin & Tkachev (1969); (2) Kato *et al.* (1979); (3) Vigdorchik *et al.* (1986); (4) Brixner *et al.* (1985); (5) Christensen (1972); (6) Schleid (1992); (7) Schleid (1991); (8) Lissner & Schleid (1992); (9) Range *et al.* (1990); (10) Stålhandske *et al.* (1985).

(= O, N) into tetrahedral interstices leads to distortions of the metal arrays caused by the nonbonded anion···anion repulsions.

Fig. 7 shows two topologically identical layers built from double edge-sharing anion-centered metal tetrahedra. The layer shown in Fig. 7(a) is a '(111)-derivative' of the fluorite framework. However, in real structures the geometry shown in Fig. 7(b) is preferred. This can be seen from comparison of the $t'':t'$ ratios in both layers. Clearly, $t'':t'$ is equal to $2/3^{1/2}$ (1.155) and 1 for the layers shown in Figs. 7(a) and 7(b), respectively. Table 5 lists inorganic compounds containing tetrahedral layers of this topology. Analysis of $t'':t'$ ratios shows that these values (1.003–1.049) are closer to 1. Apparently, a departure from the idealized form of the '(111)-derivative' layer (Fig. 7a) arises through rotation of the $[X_2A_6]$ double tetrahedra around axes perpendicular to the plane of the layer. There is little doubt that this rotation is caused by the tendency of anion-centered metal tetrahedra to have $X\cdots X$ contacts as long as possible (dotted lines in Fig. 7). This example shows that anion···anion repulsions influence the global geometry of anion-stuffed metal arrays.
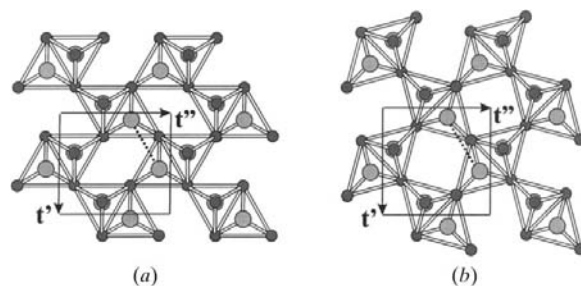

Fig. 6. Frameworks of (a) corner-sharing *stellae octangulae* and (b) corner-sharing *stellae quadrangulae*.

Fig. 7. Distortion of a layer based on anion-centered metal tetrahedra as a result of anion–anion nonbonded repulsions (anion···anion contacts are shown as dotted lines).

Table 6. *Interatomic metal–metal and anion–anion distances (Å) in structural units based on edge-sharing anion-centered metal tetrahedra and metal–metal distances in pure metals*

Metal–metal distances: $A_s \cdots A_s$ is across a shared edge. Distances shorter than $A \cdots A_{\mathrm{metal}}$ are given in bold. $\langle A \cdots A \rangle$ is the mean metal–metal distance in the metal tetrahedra. $A \cdots A_{\mathrm{metal}}$ is $2r_{\mathrm{met}}$, where r_{met} is the metallic radius given by Bokii (1971).

Compound	Figure	$A_s \cdots A_s$	$\langle A \cdots A \rangle$	$\langle X \cdots X \rangle$	$A \cdots A_{\mathrm{metal}}$	Reference
$[Pb_2O](SO_4)$	3(f)	3.58, 3.65	3.76	2.85	3.50	(1)
$[Pb_3O](UO_5)$	5(c)	3.61	3.77	2.87	3.50	(2)
$K_2[Cu_3O](SO_4)_3$	5(c)	2.81	3.15	2.71	2.56	(3)
$NaK[Cu_3O](SO_4)_3$	5(c)	2.80	3.15	2.68	2.56	(4)
$Cu[Cu_3O](SeO_3)_3$ (monoclinic)	5(c)	2.80, 2.82	3.13	2.69	2.56	(5)
$Cu[Cu_3O](SeO_3)_3$ (triclinic)	5(c)	2.81	3.14	2.69	2.56	(5)
$[Cu_4O_2][(As,V)O_4]Cl$	3(f)	2.80, 2.86	3.14	2.66	2.56	(6)
$[La_2O][TiO_4]$	3(b)	3.84	3.93	3.08	3.74	(7)
$[La_5O_3]_2In_6S_{17}$	3(c)	3.82	3.93	2.98	3.74	(8)
$[La_4O_3][AsS_3]_2$	3(h)	3.75, 3.79	3.89	2.95	3.74	(9)
$CsNa[La_3N]_2Br_{14}$	5(c)	**3.72**	3.87	3.19	3.74	(10)
$[La_3N]Br_6$	5(c)	**3.72**	3.89	3.25	3.74	(10)
$[La_8N_3O]Br_{13}$	3(f)	**3.58, 3.61**	3.88	3.09	3.74	(11)
$[Pr_3O](GeO_4)(PO_4)$	5(c)	**3.63**	3.79	3.01	3.64	(12)
$Na[Pr_4O_2]Cl_9$	3(f)	**3.60**, 3.66	3.82	2.91	3.64	(13)
$K[Pr_4O_2]Cl_9$	3(f)	**3.60**, 3.69	3.83	2.92	3.64	(13)
$Na_2[Pr_4NO]Br_9$	3(f)	**3.54, 3.57**	3.81	3.00	3.64	(14)
$[Pr_8N_3O]Br_{13}$	3(f)	**3.51–3.56**	3.81	3.03	3.64	(14)
$[Pr_2N]Cl_3$	3(f)	**3.51**	3.79	3.05	3.64	(15)
$[Gd_2O](SiO_4)$	7(b)	**3.52**	3.76	2.95	3.58	(16)
$[Gd_2O](GeO_4)$	7(b)	**3.57**	3.77	3.01	3.58	(17)
$Gd[Gd_3O_2](WO_5)_2$	3(g)	3.63–3.71	3.77	2.78	3.58	(18)
$[Gd_3N]Cl_6$	5(c)	**3.45**	3.70	3.04	3.58	(19)
$[Gd_2N]Cl_3$	3(f)	**3.35**	3.70	3.07	3.58	(20)

References: (1) Sahl (1970); (2) Sterns *et al.* (1986); (3) Starova *et al.* (1991); (4) Scordari & Stasi (1990); (5) Effenberger & Pertlik (1986); (6) Starova *et al.* (1998); (7) Guillen *et al.* (1966); (8) Gastaldi *et al.* (1982); (9) Palazzi & Jaulmes (1981); (10) Lulei (1998b); (11) Lulei (1998a); (12) Dzhurinskii *et al.* (1991); (13) Mattfeld & Meyer (1994); (14) Lulei *et al.* (1995); (15) Uhrlandt & Meyer (1995); (16) Smolin & Tkachev (1969); (17) Brixner *et al.* (1985); (18) Tyulin & Efremov (1987); (19) Simon & Koehler (1986); (20) Schwanitz-Schüller & Simon (1985).

Interestingly, structural units based on anion-centered metal tetrahedra may be distorted by the anions which are external to their structure. For instance, the chain shown in Fig. 3(f) may be bent by large halide anions (Cl, Br, I), as demonstrated by Krivovichev & Filatov (1998) and Starova *et al.* (1998).

3.2. *The matrix effect and its consequences: distortions of local geometry*

The distortions of local geometry caused by the anion$\cdots$anion repulsions may be interpreted as stretching or compressing of $A \cdots A$ contacts within the (XA_4) tetrahedron.

The main factor which causes changes in the $A \cdots A$ distances is sharing of one $A-A$ edge between two (XA_4) tetrahedra. Table 6 lists $A \cdots A$ distances in selected inorganic compounds containing tetrahedral units with edge sharing only. These units are also shown in Figs. 3, 5 and 7. As may be seen from the data in Table 6, the $A_s \cdots A_s$ metal–metal distances corresponding to the shared edges are always shorter than the others and are sometimes the same as in the metals or even shorter. The extremely short length of the shared edge is usually explained by the repulsions between central anions – known as the matrix effect in metal-rich cluster compounds (Corbett, 1981, 1996; Lulei & Corbett, 1995). The idea is that metal–metal distances (and partially metal–metal bonds) are dictated by the nonbonded anion–anion contact distances, which may be characterized by nonbonded or van der Waals radii. Table 6 also gives mean $\langle X \cdots X \rangle$ distances in the compounds considered. It can be seen that the O$\cdots$O distances are in the range 2.66–3.08 Å, whereas the N$\cdots$N distances are in the range 3.04–3.25 Å. It is noteworthy that the shortest distances are more satisfactorily described by the van der Waals contact distances [O$\cdots$O 2.80 (Pauling, 1960) or 2.58 (Zefirov & Zorkii, 1974), N$\cdots$N 3.00 Å (Pauling, 1960; Zefirov & Zorkii, 1974)] than by the nonbonded distances [2.24 and 2.28 Å, respectively (O'Keeffe & Hyde, 1981)]. The matrix effect caused by interstitial N atoms is greater than that by O atoms, evidently owing to the greater $X \cdots X$ nonbonded repulsive forces.

The compressing of one or more edges caused by their sharing leads to the stretching of other edges so that the mean $\langle A \cdots A \rangle$ distance remains approximately the same in the compounds of a given metal. This means that if metal atoms are bonded (as in metals or alloys), insertion of anions into the tetrahedral interstices leads to breaking of one sort of metal–metal bond and promotes the formation of others.

Table 7. *Tetrahedrally packed metal radii (r_{tp}) for the most widespread metals in anion-centered metal tetrahedra compared with their atomic and metallic radii*

$N(A \cdots A)$ is the number of $A \cdots A$ distances taken into account in the derivation of the r_{tp} value. Atomic radii are taken from Slater (1964); metallic radii are taken from Bokii (1971).

Atom	$N(A \cdots A)$	r_{tp} (Å)	Atomic radius (Å)	Metallic radius (Å)
Cu	168	1.57	1.35	1.28
Pb	450	1.87	1.80	1.75
Bi	180	1.92	1.60	1.82
Y	60	1.81	1.80	1.80
La	186	1.95	1.95	1.87
Ce	90	1.92	1.85	1.82
Pr	72	1.91	1.85	1.82
Nd	174	1.91	1.85	1.82
Sm	96	1.89	1.85	1.80
Eu	36	1.88	1.85	2.04
Gd	66	1.86	1.80	1.79
Tb	54	1.85	1.75	1.78
Yb	36	1.84	1.75	1.93

In order to study the relationship between $A_s \cdots A_s$ distances and mean $\langle A \cdots A \rangle$ distances in (XA_4) tetrahedra in compounds with oxocentered metal tetrahedra, we analyzed 118 symmetry-independent homometallic tetrahedra from 84 accurately determined structures. This analysis gave a correlation with coefficient $R^2 = 0.96$ (Fig. 8),

$$\langle A_s \cdots A_s \rangle = 1.275 \langle A \cdots A \rangle - 1.16 \quad (1)$$

(values in Å).

This expression allows the calculation of the possible distortions in $A \cdots A$ distances in oxocentered metal tetrahedra with known type of linkage. If n $A \cdots A$ edges are shared and compressed the other $(6 - n)$ edges are therefore stretched and may be estimated by

$$[A_{ns} \cdots A_{ns}] = [1.16n + \langle A \cdots A \rangle \times (6 - 1.275n)]/(6 - n) \quad (2)$$
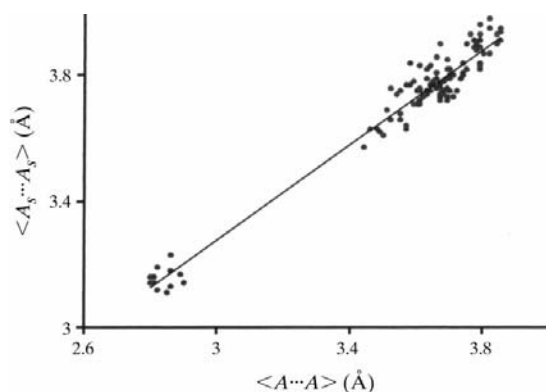
(values in Å).

Fig. 8. The dependence of the $A_s \cdots A_s$ length of the shared edge on the average $A \cdots A$ length of edges in anion-centered (XA_4) metal tetrahedra.

It should be noted that (1) and (2) give the average values only and may be used only for oxocentered metal tetrahedra. The $\langle A \cdots A \rangle$ distance for the calculations should be taken from a given set of tabulated values.

4. Rationalization of the model: introducing the set of tetrahedrally packed metal radii

One can describe the eutactic metal arrays as closest packings of equal spheres assuming metal atoms to be spheres which are elastic enough to contract on short contacts and expand on long contacts. To rationalize this model we may characterize these 'elastic' spheres by certain diameters determined on the basis of known structures containing anion-centered metal tetrahedra. We propose that they are called tetrahedrally packed metal diameters (or radii), d_{tp} (r_{tp}), to indicate their applicability at present only to one group of inorganic compounds, namely, those containing metal tetrahedra centered by O and/or N atoms.

At first it should be noted that the $A \cdots A$ distances are approximately the same for O- and N-centered metal tetrahedra. Table 6 gives mean $A \cdots A$ distances in some inorganic compounds with X-centered rare-earth metal tetrahedra. It can be seen that these distances are nearly the same within the accuracy of the analysis (0.05–0.10 Å). Therefore, the possible set of diameters (or radii) could be applied equally to O-centered and to N-centered tetrahedra.

In order to find appropriate values for the $A \cdots A$ contacts, we have analyzed only homometallic (XA_4) tetrahedra, *i.e.* those in which all A atoms are of one type. Each symmetry-independent (XA_4) tetrahedron has been analyzed separately by the calculation of the mean $\langle A \cdots A \rangle$ distance. Fig. 9 shows the distribution of 75 mean $\langle Pb \cdots Pb \rangle$ distances (calculated from 450 $Pb \cdots Pb$ contacts) in (OPb$_4$) tetrahedra. It has a maximum at 3.74–3.75 Å giving r_{tp}(Pb) = 1.87 Å. Table 7

Table 8. *Observed and calculated $\langle A' \cdots A'' \rangle$ distances (Å) in inorganic compounds containing heterometallic oxo-centered tetrahedra ($OA'_n A''_{4-n}$)*

Compound	Composition of tetrahedron	$\langle A' \cdots A'' \rangle_{obs}$	$\langle A' \cdots A'' \rangle_{calc}$	Reference
$[Bi_4Cu_3O_6](VO_4)_2$	$[OBi_2Cu_2]$	3.50	3.49	(1)
$[BiCu_2O_2](PO_4)$	$[OBi_2Cu_2]$	3.53	3.49	(2)
$A_2[Bi_2Cu_3O_4](AsO_4)_2(H_2O)$ $(A = Na, K)$	$[OBi_2Cu_2]$	3.31	3.49	(3)
$[BiCu_3O_2](SeO_3)_2Cl_2$	$[OBiCu_3]$	3.49	3.49	(4)
$[Bi_{13.333}Cu_2O_{16}](SO_4)_6$	$[OBi_3Cu]$	3.36	3.49	(5)
$[BiPbO_2]Cl$	$[OBi_2Pb_2]$	3.81	3.79	(6)
$[BiPbO_2]I$	$[OBi_2Pb_2]$	3.88	3.79	(7)
$[BiPbO](VO_4)$	$[OBi_2Pb_2]$	3.82	3.79	(8)
$[Pb_2Cu_3O_2](NO_3)_2(SeO_3)_2$	$[OPbCu_3]$	3.44	3.44	(9)
$[Eu_4Pb_6O_9](PO_4)_2$	$[OEu_2Pb_2]$	3.73	3.75	(10)
$[EuPb_2O_2][AlO_2]$	$[OEuPb_3]$	3.95	3.75	(11)

References: (1) Deacon *et al.* (1994); (2) Abraham *et al.* (1994); (3) Effenberger & Miletich (1995); (4) Pring *et al.* (1990); (5) Aurivillius (1991); (6) Gillberg (1961); (7) Ketterer & Kraemer (1985); (8) Wang & Li (1985); (9) Effenberger (1986); (10) Palkina *et al.* (1997); (11) Müller-Buschbaum & Werner (1996).

lists the set of r_{tp} values obtained by a similar procedure for A = Cu, Pb, Bi, and rare-earth metals, which are the most frequently observed A elements in compounds containing (XA_4) tetrahedra. It should be particularly emphasized that the values given in Table 7 correspond to the *average* $A \cdots A$ distance in a given (XA_4) tetrahedron. $A \cdots A$ distances within one tetrahedron may deviate essentially from these values owing to the matrix effect described above. Unfortunately, for most of the metals the data used to derive the r_{tp} values were relatively poor and therefore the values given will need to be modified as more materials are examined. We estimate the accuracy of the system to be 0.10 Å.

Comparison of tetrahedrally packed metal radii with atomic and metallic radii (Table 7) shows that insertion of anions into the tetrahedral interstices of a metal fragment causes a slight expansion (excluding A = Y, Eu, and Yb). As noted by Lebedev (1970), this is a general observation since the tetrahedral sites are smaller than the octahedral sites.

5. Application of tetrahedrally packed metal radii: heterometallic oxocentered tetrahedra

The utility of these radii may be tested easily in heterometallic anion-centered tetrahedra ($XA'_n A''_{4-n}$), *i.e.* those built from metal atoms of two sorts, A' and A''. This test provides an excellent opportunity for evaluating the proposed model. Table 8 gives the observed and calculated $\langle A' \cdots A'' \rangle$ distances in inorganic compounds containing heterometallic oxocentered tetrahedra. It can be seen that the differences between $\langle A' \cdots A'' \rangle_{obs}$ and $\langle A' \cdots A'' \rangle_{calc}$ are within 0.15 Å. Maximal deviations from the value calculated from the r_{tp} radii are observed for $A_2[Bi_2Cu_3O_4](AsO_4)_2(H_2O)$ (A = Na, K; Effenberger & Miletich, 1995), 0.18 Å, and for $[EuPb_2O_2][AlO_2]$ (Müller-Buschbaum & Werner, 1996), 0.20 Å. The latter is easily explained by the fact that in the corresponding (OPb_3Eu) tetrahedra three

Pb—Pb edges are shared, whereas three Eu—Pb edges are unshared and are therefore longer. Taking into account the fact that $r_{tp}(Pb)$ and $r_{tp}(Eu)$ are approximately the same (1.87 and 1.88 Å, respectively), we may calculate the mean metal–metal distance in the tetrahedra: 3.76 Å. This value is very close to $r_{tp}(Pb) + r_{tp}(Eu)$ = 3.75 Å. However, the reason why the Bi $\cdots$ Cu distances in $A_2[Bi_2Cu_3O_4](AsO_4)_2(H_2O)$ (A = Na, K) are shorter than the calculated value remains unclear.

6. Discussion

Many observations of metal- and alloy-like metal arrays in inorganic compounds, including those described above, raise certain intriguing questions about the reason for this phenomenon. There are a number of cluster and metal-rich compounds which can be considered as metals with small amounts of nonmetal atoms in interstices. However, in these compounds metal–metal bonding is evident because there are valence electrons disposable for this purpose. These electrons are delocalized within metal arrays and their number is governed by certain electron counting rules. In most units based on anion-centered metal tetrahedra
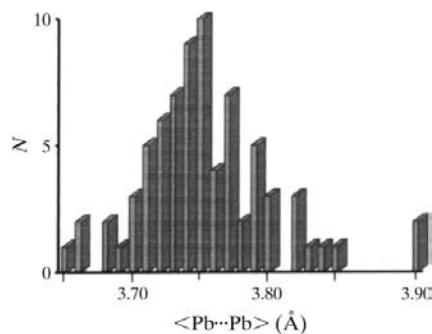

Fig. 9. The distribution of mean Pb $\cdots$ Pb distances for (OPb_4) tetrahedra in inorganic compounds.

there are no electrons available for metal–metal bonding. However, there are exceptions. Comparing the two compounds $Na_2[Pr_4O_2]Cl_9$ and $Na_2[Pr_4NO]Br_9$, based on single chains of edge-sharing anion-centered Pr tetrahedra, Lulei & Corbett (1995) noted that "crystals of $Na_2Pr_4Cl_9O_2$ with the formulation $(Na^+)_2(Pr^{3+})_4(Cl^-)_9(O^{2-})_2(e^-)$ are black because of the surplus electron, and the compound can therefore be viewed as 'reduced', while $Na_2Pr_4Br_9NO$ with the precise electron count $(Na^+)_2(Pr^{3+})_4(Br^-)_9(N^{3-})(O^{2-})$ crystallizes as green, transparent crystals and is an insulator or 'simple' salt. However, the two compounds are isostructural with similar metal–metal distances within chains forming by edge-sharing tetrahedra centered by either O or disordered O and N, respectively". As this example shows, the presence of delocalized electrons in cluster compounds leads to the appearance of certain physical properties (*e.g.* conductivity, magnetic susceptibility and color of the compound).

As mentioned previously, in some of the compounds described above the metal–metal distances are close to those in the pure metals. Numerous additional examples of this phenomenon were collected by Vegas and coauthors (see Isea *et al.*, 1998, and references therein). At the same time, the compounds considered have no electrons left for metal–metal bonding in the classical sense and therefore are considered as 'structures on the border between salts and clusters' or 'closed-shell cluster compounds' (Lulei *et al.*, 1995). They have usually been understood 'in the light of a complete valence electron transfer from metal atoms to anions' (Vegas & Martínez-Cruz, 1995). The question arises of the controversy formulated by Vegas & Martínez-Cruz (1995) as follows: 'if all the valence electrons of metal atoms are transferred to the anions, the metal structure would become broken down into atoms (cations) and it does not seem probable that they recombine, in the compound, reproducing both the topology and bond lengths of the neutral atoms in the element'.

In order to explain this controversy, Vegas & Martínez-Cruz (1995) assumed that 'in most inorganic compounds an incomplete redox process occurs and that the partial valence electrons which remain in the cations could give rise to cation–cation bonding interactions'. However, the nature of these interactions is far from being completely understood. Since they imply an attraction between closed-shell ions having the same nominal charge, they are usually called closed-shell interactions. According to Pyykkö (1997), these interactions 'are weaker than most covalent or ionic bonds but stronger than other van der Waals bonds, and roughly comparable in strength with typical hydrogen bonds'. The closed-shell interactions were repeatedly detected in the electron density distributions in normal-valent compounds as bond paths or residual electron density peaks both between cations and between anions

(Luaña, Costales & Pendás, 1997; Bader, 1998; Luaña *et al.*, 1999). As pointed out by Bader (1998), in the framework of the *Atoms in Molecules* theory (Bader, 1990) the closed-shell interactions (as well as shared interactions usually associated with one pair of electrons per bond according to the Lewis model) result from the pairing of the densities of opposite-spin electrons.

We believe that the closed-shell metal–metal interactions play a considerable role in the stabilization of anion-centered metal tetrahedra. However, our data are inadequate for a full asssessment of the problem. The most interesting results were obtained by Hoffmann and coworkers for oxocentered Pb tetrahedra (OPb_4) by means of extended Hückel calculations. Trinquier & Hoffmann (1984) showed that Pb—Pb bonding interactions do influence the structural and physical properties of the divalent lead oxides, which consist solely of (OPb_4) tetrahedra. Bengtsson & Hoffmann (1993) demonstrated the existence of Pb—Pb bonding in the isolated (OPb_4) tetrahedron (Fig. 5*a*), double $[O_2Pb_6]$ tetrahedron (Fig. 5*c*) and $[O_4Pb_8]$ *stella quadrangula* (Fig. 5*h*). Krivovichev (1999) showed that the Pb—Pb attractions cause O—Pb^{II} bond strain and influence the O—Pb^{II} bond-valence parameters within (OPb_4) tetrahedra. As for rare-earth metal tetrahedra, Hill & Catlow (1993) performed calculations for the fluorite-related cerium oxide CeO_2 using the restricted Hartree–Fock periodic algorithm which reveal the presence of Ce—Ce bonding.

Another question is why the metal fragments have different form and extent in different structures. The possible answer is that metal fragments have to accommodate distinct units or ions which may prevent their growth into complexes of higher dimensions. Two examples of the accommodation of complex tetrahedral anions ($A'O_4$) by layers of (OPb_4) tetrahedra are shown in Fig. 10 (compare with Fig. 2). It may be assumed that during the condensation of oxide-metal arrays, the ($A'O_4$) tetrahedra are avoided by including them within
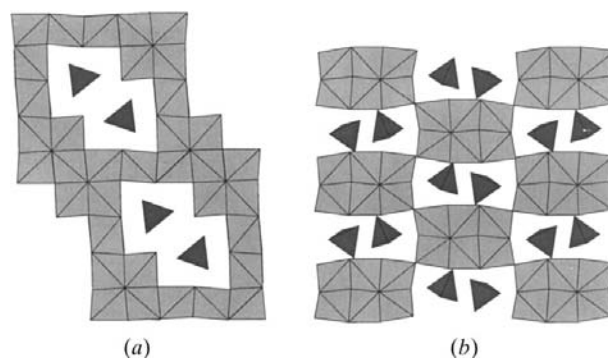

Fig. 10. The accommodation of single cation-centered ($A'O_4$) tetrahedra (dark gray) by the layers of (OPb_4) tetrahedra (light gray) in (*a*) kombatite, $[Pb_{14}O_9](VO_4)_2Cl_4$ (Cooper & Hawthorne, 1994), and (*b*) $Pb_3O_3(GeO_4)$ (Kato, 1979).

large holes. Some other observations of similar structures have been collected by Krivovichev & Filatov (1999).

References

Abraham, F., Ketatni, M., Mairesse, G. & Mernari, B. (1994). *Eur. J. Solid State Inorg. Chem.* **31**, 313–323.

Abraham, F., Thomas, D. & Nowogrocki, G. (1975). *Bull. Soc. Fr. Mineral. Cristallogr.* **98**, 25–29.

Abraham, F., Trehoux, J. & Thomas, D. (1978). *Mater. Res. Bull.* **13**, 805–810.

Abraham, F., Trehoux, J. & Thomas, D. (1979). *J. Less Common Met.* **63**, 57–63.

Adachi, G. & Imanaka, N. (1998). *Chem. Rev.* **98**, 1479–1514.

Andersson, S. (1981). *Structure and Bonding in Crystals*, Vol. 2, edited by M. O'Keeffe and A. Navrotsky, pp. 233–258. New York: Academic Press.

Aurivillius, B. (1991). *Acta Chem. Scand.* **45**, 769–774.

Bader, R. F. W. (1990). *Atoms in Molecules – A Quantum Theory.* Oxford University Press.

Bader, R. F. W. (1998). *J. Phys. Chem. A*, **102**, 7314–7323.

Beck, U. & Simon, A. (1997). *Z. Anorg. Allg. Chem.* **623**, 1011–1016.

Belov, N. V. (1976). *Ocherki Struckturnoi Mineralogii (Essays in Structural Mineralogy).* Moscow: Nedra. (In Russian.)

Bengtsson, L. & Hoffmann, R. (1993). *J. Am. Chem. Soc.* **115**, 2666–2676.

Bokii, G. B. (1971). *Kristallokhimiya (Crystal Chemistry).* Moscow: Nauka. (In Russian.)

Borisov, S. V., Bliznyuk, N. A., Kuklina, E. S., Podberezskaya, N. V. & Yudanova, T. S. (1993). *Zh. Strukt. Khim.* **34**, 116–125.

Borisov, S. V. & Podberezskaya, N. V. (1984). *Stabilnie kationnie karkasy v strukturah ftoridov I oksidov (Stable Cationic Frameworks in Fluoride and Oxide Structures).* Novosibirsk: Nauka. (In Russian.)

Borisov, S. V., Podberezskaya, N. V., Pervukhina, N. V. & Magarill, S. A. (1998). *Z. Kristallogr.* **213**, 253–258.

Bourdet, J. B., Chevalier, R., Fournier, J. P., Kohlmuller, R. & Omaly, J. (1982). *Acta Cryst.* B**38**, 2371–2374.

Braun, T. P., Simon, A., Ueno, F. & Böttcher, F. (1995). *Angew. Chem. Int. Ed. Engl.* **34**, 567–569.

Braun, T. P., Simon, A., Ueno, F. & Böttcher, F. (1996). *Eur. J. Solid State Inorg. Chem.* **33**, 251–264.

Brixner, L., Calabrese, J. & Chen, H. Y. (1985). *J. Less Common Met.* **110**, 397–410.

Carre, D., Guittard, M., Jaulmes, S., Mazurier, A., Palazzi, M., Pardo, M. P., Laurelle, P. & Flahaut, J. (1984). *J. Solid State Chem.* **55**, 287–292.

Champarnaud-Mesjard, J.-C., Frit, B., Aftati, A. & El Farissi, M. (1995). *Eur. J. Solid State Inorg. Chem.* **32**, 495–504.

Christensen, A. N. (1972). *Acta Chem. Scand.* **26**, 1955–1960.

Cooper, M. & Hawthorne, F. C. (1994). *Am. Mineral.* **79**, 550–554.

Corbett, J. D. (1981). *J. Solid State Chem.* **37**, 335–351.

Corbett, J. D. (1996). *J. Chem. Soc. Dalton Trans.* pp. 575–587.

Cotton, A. & Rice, C. E. (1978). *J. Solid State Chem.* **25**, 137–142.

Deacon, G. B., Gatehouse, B. M. & Ward, G. N. (1994). *Acta Cryst.* C**50**, 1178–1180.

Dzhurinskii, B. F., Tananaev, I. V., Tselebrovskaya, E. G. & Prozorovskii, A. I. (1991). *Izv. Akad. Nauk SSSR Neorg. Mater.* **27**, 334–339.

Effenberger, H. (1986). *Monatsh. Chem.* **117**, 1099–1106.

Effenberger, H. & Miletich, R. (1995). *Z. Kristallogr.* **210**, 421–426.

Effenberger, H. & Pertlik, F. (1986). *Monatsh. Chem.* **117**, 887–896.

Facer, G. R., Elcombe, M. M. & Kennedy, B. J. (1993). *Aust. J. Chem.* **46**, 1897–1907.

Gastaldi, L., Carre, D. & Pardo, M. P. (1982). *Acta Cryst.* B**38**, 2365–2367.

Gillberg, M. (1961). *Ark. Mineral. Geol.* **2**, 565–570.

Goldberg, D. P., Caneschi, A., Delfs, C. D., Sessoli, R. & Lippard, S. J. (1995). *J. Am. Chem. Soc.* **117**, 5789–5800.

Gougeon, P., Gall, P. & McCarley, R. E. (1991). *Acta Cryst.* C**47**, 1585–1588.

Graeser, S., Schwander, H., Demartin, F., Grammaciolli, C. M., Pilati, T. & Reusser, E. (1994). *Am. Mineral.* **79**, 996–1002.

Guillen, M., Bertaut, E. F. & Neel, M. L. (1966). *C. R. Acad. Sci. Ser. B*, **262**, 962–965.

Hägg, G. (1931). *Z. Phys. Chem. Abt. B*, **12**, 33–56.

Halet, J.-F. & Saillard, J.-Y. (1997). *Struct. Bonding*, **87**, 81–110.

Häussermann, U., Svensson, C. & Lidin, S. (1998). *J. Am. Chem. Soc.* **120**, 3867–3880.

Hill, S. E. & Catlow, C. R. A. (1993). *J. Phys. Chem. Solids*, **54**, 411–419.

Hosokawa, T., Takano, M. & Murahashi, S.-I. (1996). *J. Am. Chem. Soc.* **118**, 3990–3991.

Housecroft, C. E. (1997). *Struct. Bonding*, **87**, 137–156.

Hubert, P. H., Michel, P. & Thozet, A. (1973). *C. R. Acad. Sci. Ser. C*, **276,** 1779–1781.

Isea, R., Vegas, A. & Ramos-Gallardo, A. (1998). *Acta Cryst.* B**54**, 35–40.

Ismunandar, Kennedy, B. J. & Hunter, B. A. (1996). *J. Solid State Chem.* **127**, 178–185.

Jaulmes, S., Mazurier, A. & Guittard, M. (1983). *Acta Cryst.* C**39**, 1594–1597.

Kang, Z. C. & Eyring, L. (1997). *J. Alloys Compd.* **249**, 206–212.

Kang, Z. C. & Eyring, L. (1998). *J. Alloys Compd.* **275**, 30–36.

Kato, K. (1979). *Acta Cryst.* B**35**, 795–797.

Kato, K. (1982). *Acta Cryst.* B**38**, 57–62.

Kato, K., Hirota, K., Kanke, Y., Sato, A., Ohsumi, K., Takase, T., Uchida, M., Jarchow, O., Friese, K. & Adiwidjaja, G. (1995). *Z. Kristallogr.* **210**, 188–194.

Kato, K., Sekita, M. & Kimura, S. (1979). *Acta Cryst.* B**35**, 2201–2204.

Keller, H. L. (1982). *Z. Anorg. Allg. Chem.* **491**, 191–198.

Keller, H. L. (1983). *Angew. Chem.* **95**, 318–319.

Ketterer, J. & Kraemer, V. (1985). *Mater. Res. Bull.* **20**, 1031–1036.

Klevtsova, R. F., Kozeeva, L. P. & Klevtsov, P. V. (1967). *Izv. Akad. Nauk SSSR Neorg. Mater.* **3**, 1430–1437.

Kramer, V. & Post, E. (1985). *Mater. Res. Bull.* **20**, 407–412.

Kripyakevich, P. I. (1977). *Structure Types of Intermetallic Compounds.* Moscow: Nauka.

Krivovichev, S. V. (1999). *Z. Kristallogr.* **214**. In the press.

Krivovichev, S. V. & Filatov, S. K. (1998). *Z. Kristallogr.* **213**, 316–318.

Krivovichev, S. V. & Filatov, S. K. (1999). *Am. Mineral.* **84**. In the press.

Krivovichev, S. V., Filatov, S. K. & Semenova, T. F. (1998). *Russ. Chem. Rev.* **67**, 137–155.

Krivovichev, S. V., Filatov, S. K., Semenova, T. F. & Rozhdestvenskaya, I. V. (1998). *Z. Kristallogr.* **213**, 645–649.

Krivovichev, S. V., Shuvalov, R. R., Semenova, T. F. & Filatov, S. K. (1999). *Z. Kristallogr.* **214**, 135–138.

Lebedev, V. I. (1969). *Ionno-Atomnye Radiusy and Ikh Znachenie dlya Geokhimii I Khimii (Ionic Atomic Radii and Their Significance for Geochemistry and Chemistry).* Izd. Leningrad University. (In Russian.)

Lebedev, V. I. (1970). *Vestnik Leningr. University*, **18**, 7–22.

Lebedev, V. I. (1978). *Zap. Vses. Mineral. Ova*, **107**, 431–441.

Lissner, F., Meyer, M. & Schleid, Th. (1996). *Z. Anorg. Allg. Chem.* **622**, 275–282.

Lissner, F. & Schleid, Th. (1992). *Z. Naturforsch. Teil B*, **47**, 1614–1620.

Lissner, F. & Schleid, Th. (1993). *Z. Anorg. Allg. Chem.* **619**, 1771–1776.

Lissner, F. & Schleid, Th. (1994). *Z. Anorg. Allg. Chem.* **620**, 2003–2007.

Lissner, F. & Schleid, Th. (1997). *Z. Anorg. Allg. Chem.* **623**, 1747–1752.

Luaña, V., Costales, A., Mori-Sánchez, P. & Pendás, A. M. (1999). *J. Phys. Chem.* In the press.

Luaña, V., Costales, A. & Pendás, A. M. (1997). *Phys. Rev. B*, **55**, 4285–4297.

Lulei, M. (1998a). *Z. Kristallogr. NCS*, **213**, 245.

Lulei, M. (1998b). *Inorg. Chem.* **37**, 777–781.

Lulei, M. & Corbett, J. D. (1995). *Angew. Chem. Int. Ed. Engl.* **34**, 2262–2264.

Lulei, M., Steinwand, S. J. & Corbett, J. D. (1995). *Inorg. Chem.* **34**, 2671–2677.

Lundgren, G., Wernfors, G. & Yamaguchi, T. (1982). *Acta Cryst.* B**38**, 2357–2361.

Mattfeld, H. & Meyer, G. (1994). *Z. Anorg. Allg. Chem.* **620**, 85–89.

Mauricot, R., Gareh, J. & Evain, M. (1997). *Z. Kristallogr.* **212**, 24–28.

Müller-Buschbaum, Hk. & Werner, J.-P. (1996). *Z. Naturforsch. Teil B*, **51**, 883–887.

Nyman, H. & Andersson, S. (1979). *Acta Cryst.* A**35**, 934–937.

O'Keeffe, M. (1977). *Acta Cryst.* A**33**, 924–927.

O'Keeffe, M. & Hyde, B. G. (1980). *Philos. Trans. R. Soc. London*, **295**, 553–623.

O'Keeffe, M. & Hyde, B. G. (1981). *Structure and Bonding in Crystals*, Vol. 1, edited by M. O'Keeffe and A. Navrotsky, pp. 227–254. New York: Academic Press.

O'Keeffe, M. & Hyde, B. G. (1985). *Struct. Bonding*, **61**, 77–144.

O'Keeffe, M. & Hyde, B. G. (1996). *Patterns and Symmetry.* Washington: Mineralogical Society of America.

Palazzi, M. & Jaulmes, S. (1981). *Acta Cryst.* B**37**, 1340–1342.

Palkina, K. K., Kuz'mina, N. E. & Dzhurinskii, B. F. (1997). *Zh. Neorg. Khim.* **42**, 1094–1097.

Pauling, L. (1960). *The Nature of the Chemical Bond*, 3rd ed. Ithaca: Cornell University Press.

Pertlik, F. (1987). *Mineral. Petrogr.* **36**, 85–92.

Ploetz, K. B. & Müller-Buschbaum, Hk. (1981). *Z. Anorg. Allg. Chem.* **480**, 149–152.

Pring, A., Gatehouse, B. M. & Birch, W. D. (1990). *Am. Mineral.* **75**, 1421–1425.

Pyykkö, P. (1997). *Chem. Rev.* **97**, 597–636.

Range, K. J., Lange, K. G. & Gietl, A. (1990). *J. Less Common Met.* **158**, 137–145.

Sahl, K. (1970). *Z. Kristallogr.* **132**, 99–117.

Scheikowski, M. & Müller-Buschbaum, Hk. (1993). *Z. Anorg. Allg. Chem.* **619**, 1755–1758.

Schleid, Th. (1991). *Z. Anorg. Allg. Chem.* **602**, 39–47.

Schleid, Th. (1992). *Eur. J. Solid State Inorg. Chem.* **29**, 1015–1028.

Schleid, Th. (1996). *Eur. J. Solid State Inorg. Chem.* **33**, 227–240.

Schleid, Th. & Lissner, F. (1994). *Z. Naturforsch. Teil B*, **49**, 340–346.

Schleid, Th. & Meyer, M. (1996). *Z. Kristallogr.* **211**, 187.

Schwanitz-Schüller, U. & Simon, A. (1985). *Z. Naturforsch. Teil B*, **40**, 705–709.

Scordari, F. & Stasi, F. (1990). *Neues Jahrb. Mineral. Abh.* **161**, 241–253.

Shannon, R. D. & Calvo, C. (1973). *Acta Cryst.* B**29**, 1338–1345.

Simon, A. & Koehler, T. (1986). *J. Less Common Met.* **116**, 279–292.

Slater, J. (1964). *Quantum Theory of Molecules and Solids.* Vol. 2. New York: McGraw-Hill.

Sleight, A. W. & Bouchard, R. J. (1973). *Inorg. Chem.* **12**, 2314–2316.

Smolin, Yu. I. & Tkachev, S. P. (1969). *Kristallografiya*, **14**, 22–25.

Stålhandske, C., Aurivillius, K. & Bertinsson, G.-I. (1985). *Acta Cryst.* C**41**, 167–168.

Starova, G. L., Filatov, S. K., Fundamensky, V. S. & Vergasova, L. P. (1991). *Mineral. Mag.* **55**, 613–616.

Starova, G. L., Krivovichev, S. V. & Filatov, S. K. (1998). *Z. Kristallogr.* **213**, 650–653.

Starova, G. L., Krivovichev, S. V., Fundamensky, V. S. & Filatov, S. K. (1997). *Mineral. Mag.* **61**, 441–446.

Steele, I. M. & Pluth, J. J. (1998). *J. Electrochem. Soc.* **145**, 528–533.

Sterns, M., Parise, J. B. & Howard, C. J. (1986). *Acta Cryst.* C**42**, 1275–1277.

Trinquier, G. & Hoffmann, R. (1984). *J. Phys. Chem.* **88**, 6696–6711.

Tyulin, A. V. & Efremov, V. A. (1987). *Kristallografiya*, **32**, 371–377.

Uhrlandt, S. & Meyer, G. (1995). *J. Alloys Compd.* **225**, 171–173.

Urusov, V. S. (1989). *Zap. Vses. Mineral. Obva.* **118**, 108–119. (In Russian.)

Vassilev, P. & Nihtianova, D. (1998). *Acta Cryst.* C**54**, 1062–1064.

Vegas, A. & Isea, R. (1997). *J. Solid State Chem.* **131**, 358–362.

Vegas, A. & Isea, R. (1998). *Acta Cryst.* B**54**, 732–740.

Vegas, A. & Martínez-Cruz, L. A. (1995). *Z. Kristallogr.* **210**, 581–584.

Vigdorchik, A. G., Dem'yanets, L. N. & Malinovskii, Yu. A. (1986). *Kristallografiya*, **32**, 1381–1383.

Wang, P.-L. & Li, D.-Y. (1985). *Wu Li Hsueh Pao*, **34**, 235–240.

Wells, A. F. (1984). *Structural Inorganic Chemistry*. Oxford: Clarendon Press.

Yeom, Y. H., Kim, Y. & Seff, K. (1997). *J. Phys. Chem. B*, **101**, 5314–5318.

Zefirov, Yu. V. & Zorkii, P. M. (1974). *Zh. Strukt. Khim.* **15**, 118–122.